

Accepted Article

Title: Identification of a Pyrrole Intermediate Which Undergoes C-Glycosidation and Autoxidation to Yield the Final Product in Showdomycin Biosynthesis

Authors: Daan Ren, Minje Kim, Shao-An Wang, and Hung-wen Liu

This manuscript has been accepted after peer review and appears as an Accepted Article online prior to editing, proofing, and formal publication of the final Version of Record (VoR). This work is currently citable by using the Digital Object Identifier (DOI) given below. The VoR will be published online in Early View as soon as possible and may be different to this Accepted Article as a result of editing. Readers should obtain the VoR from the journal website shown below when it is published to ensure accuracy of information. The authors are responsible for the content of this Accepted Article.

To be cited as: *Angew. Chem. Int. Ed.* 10.1002/anie.202105667

Link to VoR: <https://doi.org/10.1002/anie.202105667>

RESEARCH ARTICLE

Identification of a Pyrrole Intermediate Which Undergoes C-Glycosidation and Autoxidation to Yield the Final Product in Showdomycin Biosynthesis

Daan Ren, Minje Kim, Shao-An Wang and Hung-wen Liu*

[*] D. Ren, M. Kim, Dr. S.-A. Wang, Prof. Dr. H.-w. Liu
Department of Chemistry, and Division of Chemical Biology and Medicinal Chemistry, College of Pharmacy, University of Texas at Austin
Austin, TX 78712 (USA)
E-mail: h.w.liu@mail.utexas.edu

Supporting information for this article is given via a link at the end of the document.

Abstract: Showdomycin is a C-nucleoside bearing an electrophilic maleimide base. Herein, the biosynthetic pathway of showdomycin is presented. The initial stages of the pathway involve non-ribosomal peptide synthetase (NRPS) mediated assembly of a 2-amino-1*H*-pyrrole-5-carboxylic acid intermediate. This intermediate is prone to air oxidation whereupon it undergoes oxidative decarboxylation to yield an imine of maleimide, which in turn yields the maleimide upon acidification. It is also shown that this pyrrole intermediate serves as the substrate for the C-glycosidase SdmA in the pathway. After coupling with ribose 5-phosphate, the resulting C-nucleoside undergoes a similar sequence of oxidation, decarboxylation and deamination to afford showdomycin after exposure to air. These results suggest that showdomycin could be an artifact due to aerobic isolation; however, the autoxidation may also serve to convert an otherwise inert product of the biosynthetic pathway to an electrophilic C-nucleotide thereby endowing showdomycin with its observed bioactivities.

Introduction

Showdomycin (**1**) along with formycin A (**2**), pyrazofurin (**3**), pseudouridine (**4**), alnumycin C1 (**5**) and minimycin (**6**) are C-nucleosides with structures characterized by a C–C ribosyl linkage between ribofuranose and a heterocyclic base (Figure 1).^[1–4] Showdomycin (**1**) isolated from *Streptomyces showdoensis*^[5] is known to inhibit DNA and RNA polymerases isolated from *Escherichia coli* leading to antibacterial and anti-tumor activities.^[7–10] It was also found to inactivate the nucleoside uptake system, and this inhibition can be reversed by nucleoside and thiol compounds such as cysteine.^[11,12] It was therefore suggested that the bioactivity of showdomycin is a consequence of its maleimide moiety, which likely acts as a Michael acceptor and thus an alkylating agent when it undergoes nucleophilic addition by a sulfhydryl group on its inhibitory targets.^[11,12] On the basis of its reactivity towards thiols, showdomycin and its synthetic derivatives have also been designed as probes for the labeling and identification of clinically important enzymes in pathogenic bacteria.^[13]

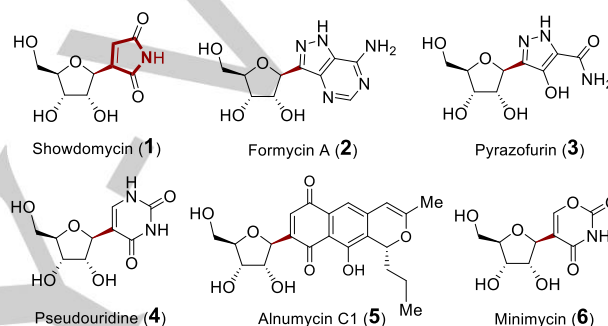


Figure 1. C-Ribosyl nucleoside antibiotics.

How the C-nucleosides are assembled in nature has been a subject of current interest. Recently, the C-glycosylation reactions in the formycin A (**2**) and pyrazofurin (**3**) biosynthetic pathways were shown to be catalyzed by ForT and PyfQ, respectively.^[14–16] Both utilize phosphoribosyl pyrophosphate (PRPP) as the ribose donor, and the reactions proceed via electrophilic aromatic substitution.^[14,16] In contrast to ForT and PyfQ, however, early studies of pseudouridine (**4**) biosynthesis showed that pseudouridine monophosphate synthase (YeiN) catalyzes C-glycosidic bond formation and cleavage between ribose 5-phosphate (**14**, R5P) and uracil through a ribose ring-opening mechanism.^[17,18] Likewise, AlnA in alnumycin C1 (**5**) biosynthesis exhibits moderate homology to YeiN and appears to catalyze the attachment of R5P to the polyketide aglycone via a mechanism involving an enediolate intermediate.^[19,20] Finally, the gene cluster for showdomycin biosynthesis (*sdm*) was recently identified in *S. showdoensis* by screening for homologs of the C-glycosidase AlnA.^[21] The corresponding C-glycosidase in showdomycin pathway has thus been hypothesized to be the gene product SdmA, and the observation that deletion of the *sdmA* gene prevents showdomycin biosynthesis *in vivo* is consistent with this hypothesis.^[21] Nevertheless, this gene assignment has not been tested *in vitro* such that the biological assembly of showdomycin remains to be definitively established.

Results and Discussion

RESEARCH ARTICLE

To address these unresolved questions, the *sdm* gene cluster was analyzed, and a cassette consisting of *sdmC*, *D*, *E*, *F* and *G* was found to be homologous to five genes in the kosinostatin (**8**) biosynthetic gene cluster (*kstB1*, *B2*, *B3*, *B4* and *B6*, respectively) (Figures 2A and 2B).^[22] Showdomycin (**1**) and kosinostatin (**8**) are both characterized by a moiety having a pyrrolidine skeleton (see ring F in **8**), and it was therefore hypothesized that construction of this moiety (e.g., **7/12** in Figure 2C) is catalyzed by the gene products of the two homologous cassettes shared by each gene cluster. This hypothesis also implies that the early steps of showdomycin biosynthesis involve nonribosomal peptide synthesis, because *sdmC* and *sdmD* (*kstB1* and *kstB2*) are annotated as encoding nonribosomal peptide synthetases (NRPS). *SdmG*, which is annotated as a transglutaminase-like protein, may then catalyze hydrolysis of the thioester linkage to release the free acid **13** as the substrate for the C-glycosidase *SdmA*. Subsequent tailoring steps including dephosphorylation, deamination, oxidation and decarboxylation would then lead to maturation of the nucleobase in showdomycin (**1**).

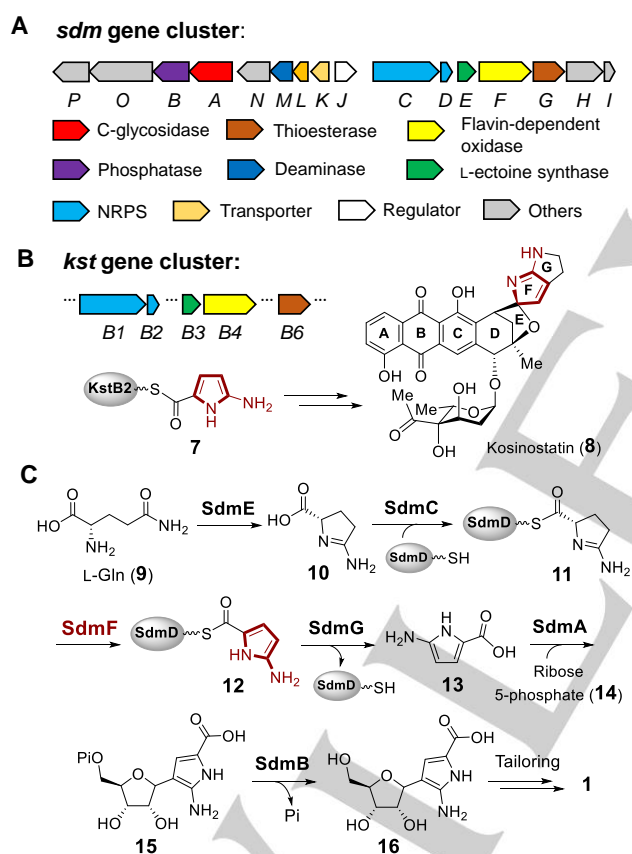


Figure 2. (A) Biosynthetic gene cluster of showdomycin in *S. showdoensis*. (B) Partial gene cluster of kosinostatin (**8**). The F ring was proposed to be biosynthesized from precursor **7**.^[22] (C) Proposed biosynthetic pathway of showdomycin (**1**).

A possible biosynthetic pathway for showdomycin biosynthesis can thus be envisaged in which a protein-tethered 2-aminopyrrole species **12** (**7** in the kosinostatin pathway) is generated via the actions of *SdmE/C/D/F* and serves as a key intermediate (see Figure 2C). The proposed pathway is likely initiated with the cyclization of L-glutamine (**9**) to **10** catalyzed by

SdmE, a homolog of L-ectoine synthase (*EctC*). Canonical *EctC* is responsible for the conversion of **17** to L-ectoine (**18**, see Figure 3A)^[23] and can also catalyze the condensation of **9** to **10** as a side reaction.^[24] *Ant24* is a homolog of *SdmE* that is similarly believed to catalyze the same reaction (i.e., **9** → **10**, see Figure 3B) during the biosynthesis of anthelvencin A (**19**) according to gene deletion and chemical complementation assays by feeding the mutant with **10**.^[25] Indeed, when 10 μM purified *SdmE* (Figure S1) was incubated with 5 mM L-glutamine in tris(hydroxymethyl)aminomethane (Tris) buffer (pH 8.0) and the reaction followed by ¹H NMR, new signals were observed consistent with a synthetically prepared standard of **10** (see Figure 3C) in support of this hypothesis. This observation is also consistent with the report that none of the 20 proteinogenic amino acids can be uploaded onto *SdmD* by *SdmC*.^[21] Thus, the conversion of L-glutamine (**9**) to **10** appears to be necessary to provide the proper substrate form recognized by the *SdmD/SdmC* NRPS system.

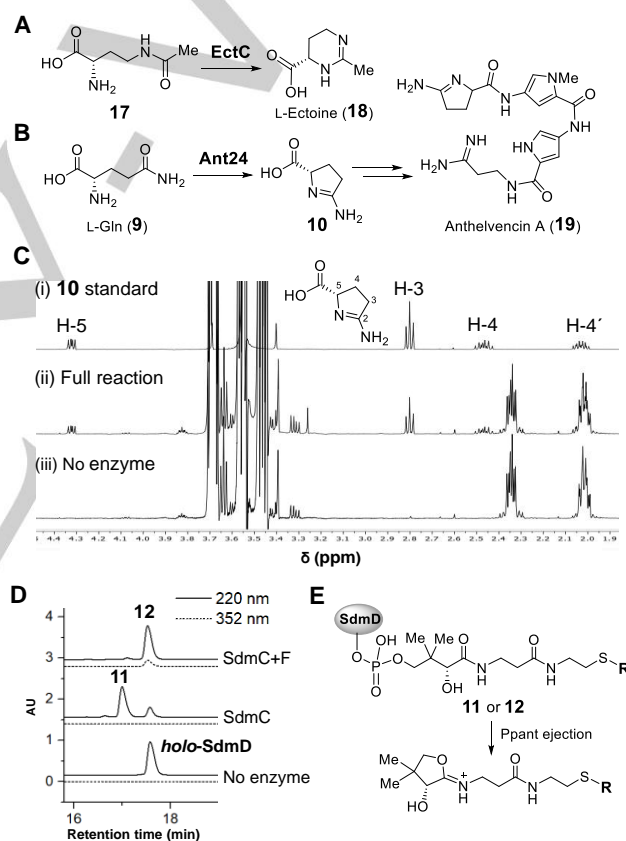


Figure 3. (A) *EctC*-catalyzed condensation of **17** to L-ectoine (**18**). (B) Biosynthesis of anthelvencin A (**19**) involving cyclization of L-Gln (**9**) to **10** by *Ant24*. (C) Monitoring product formation in the *SdmE* catalyzed reaction using ¹H NMR spectroscopy. (D) HPLC analysis of the *SdmC* and *SdmF* catalyzed reactions. *holo-SdmD* coelutes with **12**. (E) Ejection of Ppant-containing ions by MS fragmentation.^[26]

To test this hypothesis, 50 μM *apo-SdmD* was incubated with 1 mM **10** in the presence of 2 μM *SdmC*, 2 μM phosphopantetheinyl transferase (*Sfp*), 1 mM ATP, 75 μM coenzyme A, 10 mM MgCl₂ and 5 mM tris-(2-carboxyethyl)phosphine (TCEP) in 100 mM Tris buffer (pH 8.0) for 2 h. After quenching the reaction with acetonitrile, HPLC analysis of the supernatant revealed the presence of a new

RESEARCH ARTICLE

peptidyl carrier protein species (Figure 3D). To track any change at the acylation carrier site of its phosphopantetheinyl (Ppant) arm, ESI-MS was employed to detect the Ppant ion fragment ejected from the intact protein (see Figure 3E and supporting information). Indeed, an MS signal was observed for an ion fragment having the mass expected for Ppant modified with **11** (Figure S2). This implies that showdomycin biosynthesis begins with formation of the modified SdmD peptide-carrier-protein following cyclization of L-glutamine (**9** → **10** → **11**).

Formation of a 2-aminopyrrole from the 2-aminopyrrole intermediate **11** requires an oxidation reaction that may be catalyzed by SdmF, which is annotated as a flavin-dependent oxidase. When 1 μ M SdmF was included in the above assay under aerobic condition, a new species was observed by MS with a molecular weight two mass units less than **11** (Figures 3D and S2). Purification of the SdmD/SdmC/SdmF coupled reaction mixture by gel filtration led to isolation of the modified SdmD, which exhibited a UV-Vis absorption maximum at 352 nm at pH 8.0 (Figure S3). A similar spectrum with a maximum absorbance at 350 nm (pH 8.0) was also observed with a synthesized *N*-acetylcysteamine (*S*-NAc) analog of **12** (Figure S3), suggesting that the dehydrogenated product formed in the presence of SdmF is the proposed intermediate **12**, which contains a 2-aminopyrrole moiety conjugated to a thioester. Furthermore, when SdmF was incubated with **10** in the absence of SdmC and SdmD, no substrate consumption was observed by 1 H-NMR spectroscopy (Figure S4). These observations imply that SdmF catalyzes the dehydrogenation of **11** to **12** in a reaction that takes place only after loading of **10** onto the peptide-carrier-protein SdmD.

Incubation of the purified **12** with SdmG resulted in the decrease of the absorbance at 352 nm and an increase in absorbance at 288 nm with an isosbestic point at 310 nm (Figure 4A). Therefore, it was hypothesized that SdmG catalyzes the subsequent hydrolysis of **12** to generate the free 2-amino-1H-pyrrole-5-carboxylic acid **13**. However, LC-MS analysis failed to detect **13** following deproteinization of the reaction mixture via ultrafiltration, and the absorbance at 288 nm was also found to diminish over time (Figure 4B). One possible explanation for the results with SdmG and intermediate **12** is that **13** is unstable under aerobic conditions, because 2-aminopyrroles are prone to autoxidation.^[27-29] Moreover, the pyrrole-2-carboxylate intermediates identified in the biosynthesis of violacein^[30] and rebeccamycin^[31,32] have also been shown to react with oxygen resulting in oxidative decarboxylation to the corresponding oxo-products (Figure S5). These early reports suggested that **13** may undergo a similar autoxidation and subsequent decarboxylation under aerobic conditions to yield 2-iminopyrrolone **21** and maleimide **22** following SdmG catalyzed hydrolysis of **12** (Figures 4B and 4C). Given that **21** and **22** are potential Michael acceptors and *holo*-SdmD would also be released in the SdmG reaction, the free thiol of the phosphopantetheinyl arm of *holo*-SdmD may in turn react with **21** or **22** to form adducts such as **23** or **24** (Figure 4D).

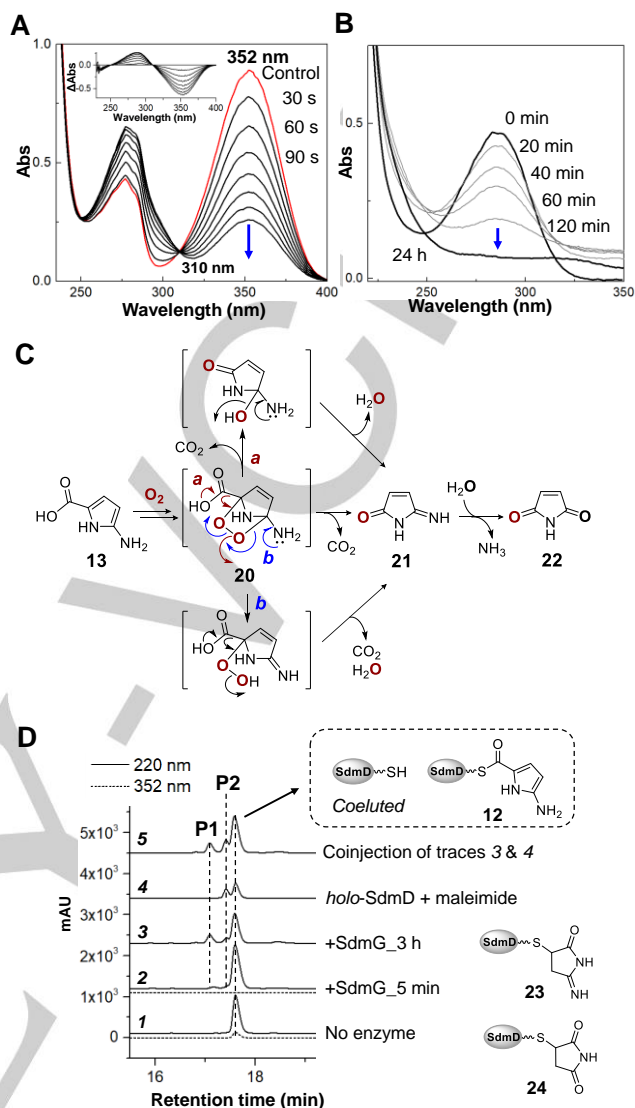


Figure 4. (A) Time-course of the SdmG-catalyzed reaction monitored by UV-Vis spectroscopy. The final enzyme and substrate concentrations were 50 nM and 30 μ M, respectively. The inset shows difference spectra calculated by subtracting the spectrum of a control with no SdmG from each time-point. (B) Decomposition of the SdmG product determined by the diminishing absorbance at 288 nm of the reaction filtrate over 24 h. (C) The proposed autoxidation of **13**. Decomposition of the endoperoxide intermediate **20** to **21** and **22** may proceed via either direct decarboxylation (route a) or O-O bond cleavage triggered by imine formation (route b). (D) HPLC analysis of the proteinaceous products from the aerobic SdmG reaction. The elution was monitored at 352 nm (dash line) to determine the consumption of substrate **12**.

In order to test these hypotheses, the SdmG assay was again performed and analyzed by LC-MS to investigate the formation of modified peptidyl carrier proteins. HPLC analysis revealed the complete disappearance of substrate **12** within 5 min as indicated by the absence of any signal at 352 nm (Figure 4D trace 2). Meanwhile, gradual formation of two new peaks **P1** and **P2** over 3 h were found as the major SdmD-bound species in the SdmG reaction (Figure 4D). MS analysis of the Ppant ejection ions of **P1** and **P2** were consistent with the proposed structures of **23** and **24** (Figure S6). Furthermore, a standard of **24** prepared by reacting maleimide with *holo*-SdmD was observed to coelute with **P2** produced in the SdmG catalyzed reaction (Figure 4D trace 5).

RESEARCH ARTICLE

Finally, when $^{15}\text{N}_2$ -L-glutamine was used in the SdmE/SdmC/SdmD/SdmF/SdmG reaction, an increase of two mass units of the Ppant ejection ion during LC-MS analysis of **P1** was observed consistent with the assigned structure **23** (Figure S7). Therefore, the observed consumption of substrate **12** and formation of **23** and **24** agrees with the proposed reaction sequence in which **13** is slowly oxidized and covalently trapped by *holo*-SdmD.

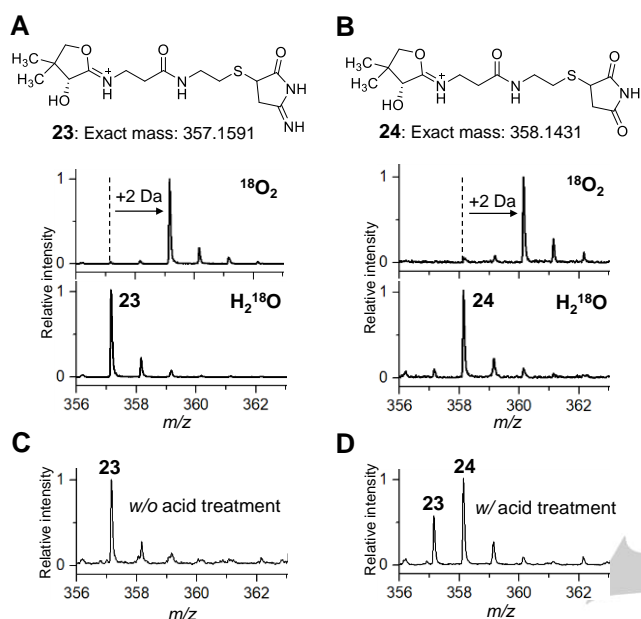


Figure 5. Ppant ejection mass spectra of adducts (A) **23** and (B) **24** in the presence of $^{18}\text{O}_2$ + natural abundance H_2O (upper trace) or natural abundance O_2 + H_2^{18}O (lower trace). (C) Ppant ejection mass spectra of SdmG reaction mixture without and (D) with excess 0.1% TFA pre-treatment.

To further investigate the mechanism by which **13** undergoes oxidative decarboxylation, 50 μM **12** was incubated with 1 μM SdmG in Tris buffer (pH 8.0) under an $^{18}\text{O}_2$ atmosphere for 3 h. A mass increase of 2 Da was observed with both **23** and **24** indicating incorporation of a single ^{18}O center from molecular oxygen to each (Figures 5A and 5B). In contrast, neither adduct contained ^{18}O when the incubation was conducted with natural abundance O_2 and ^{18}O -enriched water. The absence of ^{18}O incorporation from solvent in **24** suggested that **24** might be derived from the hydrolysis of **23** during HPLC separation and/or LC-MS analysis rather than during the assay. Indeed, **23** was found to be stable at pH 8.0 (SdmG assay conditions) but could be converted to **24** at pH 2.0 (HPLC and LC-MS conditions) as shown in Figures 5C and 5D. These results agree with the proposed transformation of **13** to **21**. In a separate experiment where the SdmG reaction was carried out anaerobically and the reaction filtrate was promptly analyzed by LC-MS, a signal consistent with **13** was observed directly (calc. m/z for $\text{C}_5\text{H}_7\text{N}_2\text{O}_2^+$ $[\text{M}+\text{H}]^+$ 127.0508; found 127.0503) along with the in-source decarboxylated fragment (calc. m/z for $\text{C}_4\text{H}_7\text{N}_2^+$ $[\text{M}-\text{CO}_2+\text{H}]^+$ 83.0609; found 83.0604) (Figure S8).

The demonstrated reactivity of **13** toward O_2 suggested that it is electron-rich and may thus serve as a nucleophile in the formation of the C-ribosyl linkage catalyzed by SdmA, which is

annotated as a C-glycosidase in the *sdm* cluster. To test this hypothesis, the *in vitro* characterization of SdmA using ribose 5-phosphate (R5P, **14**) as the electrophile was conducted under anaerobic conditions to prevent autoxidation of **13**. First, **13** was freshly prepared by incubating **12** with SdmG and then removing the enzymes by ultrafiltration. When 10 μM SdmA was added to the resulting solution containing **13** (ca. 80 μM) along with 0.8 mM R5P (**14**) and 5 mM MgCl_2 , a new species was detected by HPLC with a UV-vis absorption spectrum nearly identical to that of **13** but with a different HPLC retention time (Figures 6B and S9). HRMS analysis of this new product revealed a chemical composition of $\text{C}_{10}\text{H}_{16}\text{N}_2\text{O}_9\text{P}$, which is consistent with the structure of **15** (calc. 339.0593, found 339.0599). The in-source decarboxylated fragment was also observed by MS (calc. m/z for $\text{C}_9\text{H}_{16}\text{N}_2\text{O}_7\text{P}$ $[\text{M}-\text{CO}_2]^+$ 295.0695, found 295.0710) (Figure S10), indicating the presence of a labile carboxyl group and supporting the assignment of the SdmA product as **15**. However, similar results would also be expected for a product containing a C4-C1' linkage (i.e., **27**) rather than a C3-C1' linkage as shown in **15** (Figure 6A). While the isolation and direct characterization of **15** failed due to its instability, the regiochemistry of adduct formation was determined by using the $[4\text{-}^2\text{H}]$ -isotopolog of **13** prepared enzymatically from $[3,3\text{-}^2\text{H}_2]$ -L-glutamine. LC-MS analysis of the corresponding SdmA product showed retention of one deuterium (see Figure S11), indicating **15** rather than **27** is the enzymatic product of SdmA. This regioselectivity is also consistent with the increased nucleophilicity of C3 of **13** due to the amino substituent at the C2 position. Moreover, if SdmB, which is annotated as a phosphatase, was present in the reaction, the correct mass of the dephosphorylated product **16** was detected (calc. m/z for $\text{C}_{10}\text{H}_{15}\text{N}_2\text{O}_6$ $[\text{M}+\text{H}]^+$ 259.0930, found 259.0923) (Figure S10). Interestingly, unlike the cases of ForT and PyfQ, PRPP is not a substrate for SdmA (Figure 6B). It was also found that maleimide (**22**) could not be processed by SdmA (Figure S12). Thus, glycosidation of **13** to **15** most likely occurs prior to oxidative decarboxylation of **13**.

Given that the C-glycosylation products **15** and **16** carry the same pyrrole moiety as **13**, they may also undergo autoxidation in air to generate **29** and **31**, respectively. To trap and characterize the anticipated oxidative decarboxylation products, a coupled assay of **12** and **14** with SdmG/SdmA was conducted under aerobic conditions. When 50 μM **12** was incubated with 0.2 μM SdmG, 10 μM SdmA in the presence of 0.5 mM ribose 5-phosphate (**14**), 5 mM MgCl_2 in Tris buffer (pH 8.0), LC-MS analysis revealed the presence of two new SdmD-bound adducts **29** and **30** accompanied by a small amount of **23** and **24** due to autoxidation of the intermediate **13** (Figures 6C and S13). Adducts **29** and **30** were not detected when R5P was replaced by PRPP, which is consistent with the aforementioned results of the anaerobic assays. Moreover, when SdmB was included in the coupled reaction assay, products with the correct mass for **26** as well as showdomycin (**1**) covalently linked to *holo*-SdmD (i.e., adducts **31** and **32**, respectively, Figure S14) could be detected. To directly test if **16** can be converted to showdomycin via autoxidation, the SdmA/SdmB coupled reaction filtrate from anaerobic incubation was exposed to air for 3 h during which time the correct mass of **26** was detected (calc. m/z for $\text{C}_9\text{H}_{11}\text{N}_2\text{O}_5$ $[\text{M}-\text{H}]^-$ 227.0668, found 227.0675). When this mixture was acidified with excess 0.1% formic acid (FA) to pH \sim 3 for 2 h, LC-MS analysis revealed the presence of both showdomycin (**1**) and the C1' epimer of showdomycin (**1'-epi-1**) (Figure 6D). Two new

RESEARCH ARTICLE

peaks (**P3** and **P4**) which have the same exact mass as **1** and 1'-*epi*-**1** were also noted. These species were assigned to be pyranose isomers of showdomycin (**33** and **34**) based on their coelution with the chemically prepared standards. These observations are consistent with the proposed pathway in Figure 2C whereby **16** is a key intermediate *en route* to the observed natural product showdomycin (**1**).

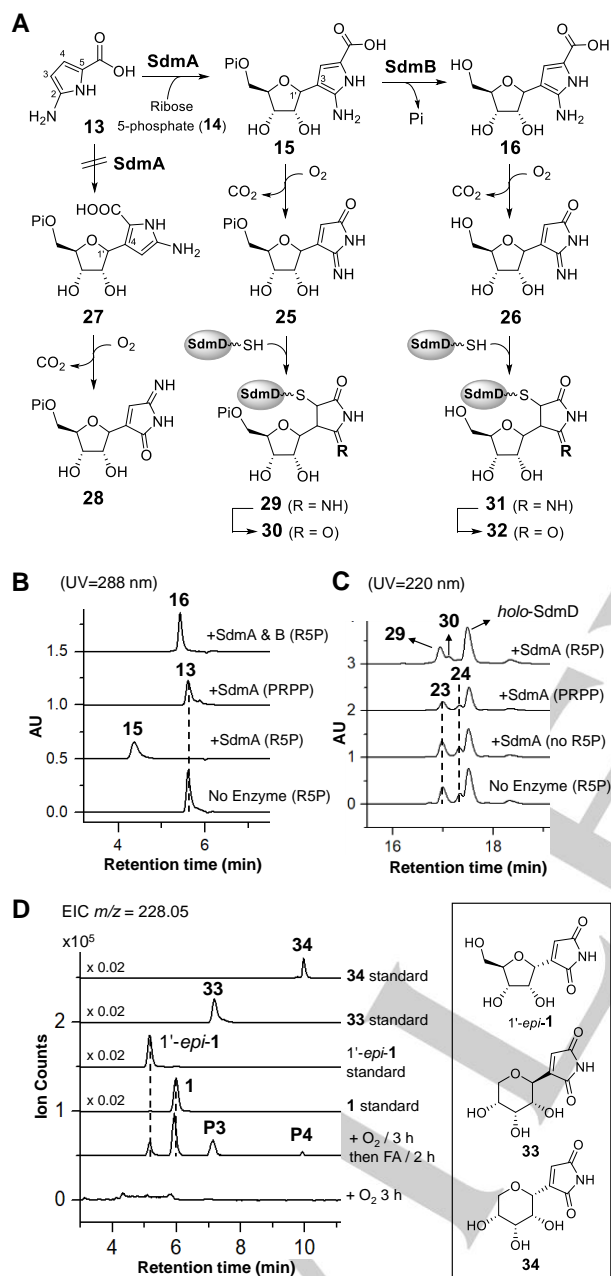


Figure 6. (A) Products generated in the reactions catalyzed by SdmA and SdmB. The nascent enzyme products **15** and **16** were susceptible to oxidative decarboxylation and covalent modification by *holo*-SdmD. (B) HPLC analysis of anaerobic incubations of SdmA and SdmB. (C) HPLC analysis of aerobic incubations of **12** and SdmA coupled with SdmG. (D) LC-MS analysis of autoxidation of **16**. Extracted ion chromatogram (EIC) traces corresponding to $[M - H]^-$ signals from **1** and 1'-*epi*-**1** are shown. The unknown **P3** and **P4** have the same exact mass as showdomycin and have the same retention time with standards of pyranose isomer of showdomycin (**33** and **34**, respectively). Proposed mechanism for the formation of 1'-*epi*-**1**, **33** and **34** is shown in Figure S15.

Conclusion

The biosynthetic pathway for showdomycin as encoded by the *sdm* gene cluster has now been reconstituted *in vitro*. The biosynthetic precursors to showdomycin are L-glutamine (**9**) and ribose 5-phosphate (**14**) with no apparent dependence on PRPP in contrast to the pyrazole C-nucleosides formycin A (**2**) and pyrazofurin (**3**).^[14-16] Assembly is initiated by SdmE catalyzed cyclization of L-glutamine to yield a 2-amino-1-pyrroline-5-carboxylate intermediate that is subsequently loaded onto the phosphopantetheine arm of the peptidyl carrier protein SdmD (**9** → **10** → **11**). Oxidation of the resulting thioester-linked pyrroline is then catalyzed by the flavoenzyme SdmF (**11** → **12**) before SdmG mediated hydrolysis to yield the free 2-amino-1*H*-pyrroline-5-carboxylate species **13** as the key intermediate. While it is unclear why an NRPS system (SdmC and SdmD) participates in producing **13**, it nevertheless is necessary as SdmF is unable to catalyze the direct oxidation of **10**. In contrast, kosinostatin biosynthesis, which involves homologs of the showdomycin SdmE, SdmC, SdmD, SdmF and SdmG enzymes, has been proposed to require further NRPS catalyzed modifications in addition to oxidation.^[22] Thus, while showdomycin and kosinostatin biosynthetic gene clusters may share a common evolutionary ancestor, further development may have led to the observed specificity of SdmF despite other NRPS functions having been lost.

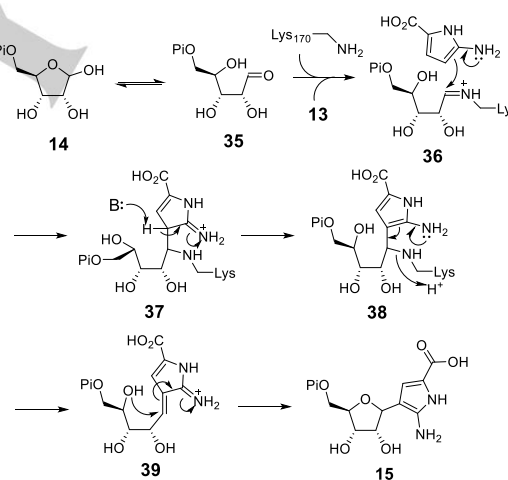


Figure 7. Proposed mechanism of glycosidic bond formation catalyzed by SdmA. Based on sequence alignment with YeiN^[17], Lys170 in SdmA is proposed to form a Schiff base with the ring-opened ribose 5-phosphate precursor (**35**) prior to the nucleophilic addition of **13**.

The key step in the showdomycin biosynthetic pathway is regioselective formation of the C–C linkage between C3 of **13** and C1' of ribose 5-phosphate (**14**) to yield **15**, which is unstable in the presence of molecular oxygen. This reaction is catalyzed by SdmA. Given the high sequence homology between SdmA and the pseudouridine monophosphate C-glycosidase YeiN (42% identity, 59% similarity) as well as their dependence on ribose 5-phosphate but not PRPP, an analogous C-glycosidation mechanism can be envisioned as depicted in Figure 7.^[17,18] Subsequent dephosphorylation catalyzed by SdmB yields the showdomycin precursor **16** that is similarly unstable towards autoxidation. Although showdomycin and 1'-*epi*-showdomycin were both detected as autoxidation products of **16**, this result

RESEARCH ARTICLE

cannot be referred to the stereochemistry of **16** or **15** without more direct evidence. This is because C-nucleosides are known to be susceptible to epimerization at C1' under acidic conditions.^[33-36]

The final tailoring steps that convert **16** to showdomycin are expected to include oxidation, decarboxylation and deamination reactions. However, the observed instability of compound **16** indicates that the final steps of showdomycin formation can proceed via a series of nonenzymatic transformations to afford **1**, 1'-*epi*-**1** and the pyranose isomers of showdomycin (**33** and **34**). Hence, the C-nucleoside **16** may actually be the true product of the showdomycin biosynthetic pathway with showdomycin itself being an artifact due to isolation under aerobic and acidic conditions. Similar examples of misidentified biosynthetic products due to oxidation, decomposition or further modifications upon isolation have also been reported in other natural product systems, making such a possibility not without precedent.^[37,38] Alternatively, the nonenzymatic conversion of **16** to showdomycin may indeed represent the final stages of the biosynthetic pathway, given that **16** is not expected to exhibit the same biological activity typically ascribed to the more electrophilic showdomycin. While these hypotheses remain to be further explored, the present results offer a full description of showdomycin biosynthesis as well as its peculiar features within the context of C-nucleoside biochemistry. Importantly, the in vitro reconstitution of showdomycin biosynthesis unveils the double-edged effect of autoxidation as it can deplete the pyrrole intermediate prior to C-glycosidation but also appears to be necessary for the putative maturation of the biologically active natural product.

Acknowledgements

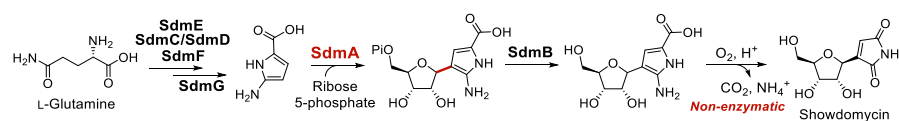
We thank Dr. Mark Ruszczycky for his critical review and help of preparing the manuscript. This work was supported by grants from the National Institutes of Health (GM040541, GM035906) and the Welch Foundation (F-1511).

Keywords: C-nucleoside • maleimide • biosynthesis • C-glycosidation • autoxidation.

- [1] R. J. Suhadolnik in *Nucleoside Antibiotics*; Wiley-Interscience: New York, **1970**.
- [2] J. G. Buchanan, *Fortschr. Chem. Org. Naturst.* **1983**, *44*, 243-299.
- [3] J. Stambaský, M. Hocek, P. Kocovský, *Chem. Rev.* **2009**, *109*, 6729-6764.
- [4] E. De Clercq, *J. Med. Chem.* **2016**, *59*, 2301-2311.
- [5] H. Nishimura, M. Mayama, Y. Komatsu, H. Kato, N. Shimaoka, Y. Tanaka, *J. Antibiot. (Tokyo)* **1964**, *17*, 148-155.
- [6] K. R. Darnall, L. B. Townsend, R. K. Robins, *Proc. Natl. Acad. Sci. U. S. A.* **1967**, *57*, 548-553.
- [7] D. Maryanka, I. R. Johnston, *FEBS Lett.* **1970**, *7*, 125-128.
- [8] P. Roy-Burman, *Recent Results Cancer Res.* **1970**, *25*, 70-82.
- [9] S. Matsuura, O. Shiratori, K. Katagiri, *J. Antibiot. (Tokyo)* **1964**, *17*, 234-237.
- [10] S. Roy-Burman, P. Roy-Burman, D. W. Visser, *Cancer Res.* **1968**, *28*, 1605-1610.
- [11] H. Nishimura, Y. Komatsu, *J. Antibiot. (Tokyo)* **1968**, *21*, 250-254.
- [12] Y. I. Uehara, J. M. Fisher, M. Rabinowicz, *Biochem. Pharmacol.* **1980**, *29*, 2199-2204.
- [13] T. Böttcher, S. A. Sieber, *J. Am. Chem. Soc.* **2010**, *132*, 6964-6972.
- [14] D. Ren, S.-A. Wang, Y. Ko, Y. Geng, Y. Ogasawara, H.-w. Liu, *Angew. Chem. Int. Ed. Engl.* **2019**, *58*, 16512-16516.
- [15] M. Zhang, P. Zhang, G. Xu, W. Zhou, Y. Gao, R. Gong, Y. S. Cai, H. Cong, Z. Deng, N. P. J. Price, X. Mao, W. Chen, *Appl. Environ. Microbiol.* **2020**, *86*, e01971-19.
- [16] S. Gao, A. Radadiya, W. Li, H. Liu, W. Zhu, V. de Crécy-Lagard, N. G. J. Richards, J. H. Naismith, *Chem. Commun. (Camb.)* **2020**, *56*, 7617-7620.
- [17] S. Huang, N. Mahanta, T. P. Begley, S. E. Ealock, *Biochemistry* **2012**, *51*, 9245-9255.
- [18] M. Pfeiffer, B. Nidetzky, *Nat. Commun.* **2020**, *11*, 6270.
- [19] T. Oja, K. D. Klika, L. Appassamy, J. Sinkkonen, P. Mäntsälä, J. Niemi, M. Metsä-Ketelä, *Proc. Natl. Acad. Sci. U. S. A.* **2012**, *109*, 6024-6029.
- [20] T. Oja, L. Niiranen, T. Sandalova, P. Mäntsälä, G. Schneider, M. Metsä-Ketelä, *Proc. Natl. Acad. Sci. U. S. A.* **2013**, *110*, 1291-1296.
- [21] K. Palmu, P. Rosenqvist, K. Thapa, Y. Ilina, V. Siitonen, B. Baral, J. Mäkinen, G. Belogurov, P. Virta, J. Niemi, M. Metsä-Ketelä, *ACS Chem. Biol.* **2017**, *12*, 1472-1477.
- [22] H.-M. Ma, Q. Zhou, Y.-M. Tang, Z. Zhang, Y.-S. Chen, H.-Y. He, H.-X. Pan, M.-C. Tang, J.-F. Gao, S.-Y. Zhao, Y. Igarashi, G.-L. Tang, *Chem. Biol.* **2013**, *20*, 796-805.
- [23] P. Peters, E. A. Galinski, H. G. Trüper, *FEMS Microbiol. Lett.* **1990**, *71*, 157-162.
- [24] E. M. Witt, N. W. Davies, E. A. Galinski, *Appl. Microbiol. Biotechnol.* **2011**, *91*, 113-122.
- [25] C. Aubry, P. Clerici, C. Gerbaud, L. Micouin, J. L. Pernodet, S. Lautru, *ACS Chem. Biol.* **2020**, *15*, 945-951.
- [26] P. C. Dorrestein, S. B. Bumpus, C. T. Calderone, S. Garneau-Tsodikova, Z. D. Aron, P. D. Straight, R. Kolter, C. T. Walsh, N. L. Kelleher, *Biochemistry* **2006**, *45*, 12756-12766.
- [27] M. De Rosa, R. P. Issac, G. Houghton, *Tetrahedron Lett.* **1995**, *36*, 9261-9264.
- [28] M. De Rosa, R. P. Issac, M. Marquez, M. Orozco, F. J. Luque, M. D. Timken, *J. Chem. Soc., Perkin Trans. 2* **1999**, *7*, 1433-1438.
- [29] C. Pichon-Santander, R. Shankar, A. I. Scott, *Tetrahedron Lett.* **1997**, *38*, 1293-1296.
- [30] K. Shinoda, T. Hasegawa, H. Sato, M. Shinozaki, H. Kuramoto, Y. Takamiya, T. Sato, N. Nikaidou, T. Watanabe, T. Hoshino, *Chem. Commun.* **2007**, *40*, 4140-4142.
- [31] A. R. Howard-Jones, C. T. Walsh, *J. Am. Chem. Soc.* **2007**, *129*, 11016-11017.
- [32] K. S. Ryan, A. R. Howard-Jones, M. J. Hamill, S. J. Elliott, C. T. Walsh, C. L. Drennan, *Proc. Natl. Acad. Sci. U. S. A.* **2007**, *104*, 15311-15316.
- [33] W. E. Cohn, *J. Biol. Chem.* **1960**, *235*, 1488-1498.
- [34] R. Sharpiro, R. W. Chambers, *J. Am. Chem. Soc.* **1961**, *83*, 3920-3921.
- [35] R. W. Chambers, V. Kurkov, R. Sharpiro, *Biochemistry* **1963**, *2*, 1192-1203.
- [36] Y. L. Jiang, J. T. Stivers, *Tetrahedron Lett.* **2003**, *44*, 85-88.
- [37] C. Huang, C. Yang, W. Zhang, L. Zhang, B. C. De, Y. Zhu, X. Jiang, C. Fang, Q. Zhang, C.-S. Yuan, H.-w. Liu, C.-s. Zhang, *Nat. Commun.* **2018**, *9*, 2088.
- [38] R. J. Capon, *Nat. Prod. Rep.* **2020**, *37*, 55-79.

RESEARCH ARTICLE

Entry for the Table of Contents



C-nucleoside biosynthesis: The biosynthetic pathway of the C-nucleoside showdomycin was reconstituted *in vitro*. Key steps include cyclization of L-glutamine to yield an oxygen-labile pyrrole intermediate that serves as the substrate for C-glycosidation catalyzed by SdmA. Autoxidative maturation of the pyrrole nucleobase to the maleimide moiety of showdomycin can then proceed non-enzymatically.